Isothermal Crystallization of High Density Polyethylene and Nanoscale Calcium Carbonate Composites

Jiann-Wen Huang

Department of Styling and Cosmetology, Tainan University of Technology, Yung Kang City, Taiwan, Republic of China

Received 11 June 2007; accepted 1 October 2007
DOI 10.1002/app.27503
Published online 26 November 2007 in Wiley InterScience (www.interscience.wiley.com).

ABSTRACT: High density polyethylene (HDPE) and calcium carbonate ($CaCO_3$) nanocomposites with maleic anhydride grafted HDPE (manPE) as a compatibilizer were prepared via compounding in a twin-screw extruder. The $CaCO_3$ are well dispersed in the HDPE matrix from the observation of transmission electron microscope. The isothermal crystallization kinetics was studied by differential scanning calorimetry and simulated by Avrami and Tobin models. The nucleation constants and fold surface free energy were estimated from Lauritzen–Hoffman relation. The results indicate that both manPE and well-dispersed $CaCO_3$ particles would act as nuclei to induce heterogeneous nucleation and enhance crystallization rate. © 2007 Wiley Periodicals, Inc. J Appl Polym Sci 107: 3163–3172, 2008

Key words: crystallization; composite; polyethylene; kinetics

INTRODUCTION

Polymer nanocomposites have attracted great attention because of their significant improvements in mechanical strength and thermal properties at low filler loadings.[1–9] High density polyethylene (HDPE) is widely used in domestic and industrial applications as a cost-effective material for its high rigidity and solvent resistance. Inorganic particles as calcium carbonate ($CaCO_3$) and silica (SiO_2) are often used when rigidity of HDPE has to be further increased. The compatibility of HDPE, however, is poor with most materials because of the lack of polar groups in the backbone. Introducing polar groups, such as maleic anhydride to the HDPE matrix,[8] modifying the filler surface,[10] are commonly used techniques to improve the compatibility of HDPE.

In addition to the rigidity-enhancing effect in a filler-polymer composite, the fillers have also been noted to influence the crystallization process.[2–5] It is worth noting that fillers can either promote or retard the crystallization of polymers, depending on the dispersion and loading content of the fillers in thermoplastic matrices.[11,12]

The effects of nanoscale $CaCO_3$ and compatibilizer on the properties and crystallization of polypropylene (PP)/$CaCO_3$ nanocomposites have been studied in detail.[4–9] Nanoscale $CaCO_3$ has been found effective in improving low temperature toughness of PP. $CaCO_3$ has also been found to affect crystallization kinetics. $CaCO_3$ can either increase or retard the crystallization rate depending on the filler size, loading content, and dispersion of the particles. Similar results are obtained for HDPE/vermiculite[1] and HDPE/clay[2,3] systems that the properties are dependent on the dispersion of fillers and crystallinity. Surface modifications of micro- and nano-scale $CaCO_3$ were found to be critical to improve the toughness of HDPE[10,13] However, few studies have been devoted to the effects of nanoscale $CaCO_3$ on the crystallization of HDPE. The knowledge relative to crystallization kinetics of HDPE/$CaCO_3$ nanocomposites is scarce.

In this work, the nanoscaled $CaCO_3$ particles were dispersed in HDPE by using maleic anhydride grafted HDPE (manPE) as a compatibilizer. In addition to the effect of manPE on the dispersion of $CaCO_3$ in HDPE, the effects of manPE and $CaCO_3$ on the crystallization behaviors of HDPE were also analyzed.

EXPERIMENTAL

Materials

Commercial grade HDPE was supplied by Formosa Plastics Corp. (Taipei, Taiwan) under trade name TAISOX® 9000 with a melt flow index (MFI) of 0.07 g/10 min (2.16 kgf, ASTM D1238). Maleic anhydride grafted HDPE (manPE) with a MFI of 12.3 g/10 min (190°C × 2.16 kgf, ASTM D1238), trade name: Fusabond® E MB265D was produced by DuPont (USA). Nanoscale $CaCO_3$ was purchased from Nanomateri-

Correspondence to: J.-W. Huang (jw.huang@msa.hinet.net).

Journal of Applied Polymer Science, Vol. 107, 3163–3172 (2008)

als Technology Co., Ltd. (Shanxi, China, and Trade Name: NPCC-201). All materials were used as received without purification.

Sample preparation

All materials were dried at 323 K in a vacuum oven for 6 h before compounding. manPE and 20 wt % nanoscale $CaCO_3$ were compounded with a twin-screw extruder (L/D = 32, D = 40 mm, Continent Machinery Company, Model CM-MTE 32) at 473 K and 300 rpm to make masterbatch. The 25 wt % masterbatch was then mixed with HDPE and re-compounded at 473 K and 300 rpm to prepare HDPE/manPE/$CaCO_3$, which contained 5 wt % $CaCO_3$, 20 wt % manPE, and 75 wt % HDPE. Two blends of HDPE/manPE and HDPE/$CaCO_3$ were also prepared with 25 wt % manPE and 5 wt % nanosized $CaCO_3$, respectively, with a twin-screw extruder at 473 K and 300 rpm. As a base of comparison, the neat HDPE was also passed through the extruder at the same conditions.

Isothermal crystallization

Crystallization behaviors of the blends were monitored with a differential scanning calorimeter, Perkin–Elmer DSC-1. The differential scanning calorimeter was calibrated using indium with sample weight of 8–10 mg. All operations were carried out in a nitrogen atmosphere. Before data collection, the samples were heated to 453 K and held in the molten state for 5 min to eliminate the influence of thermal history. The sample melts were then subsequently quenched at a rate of 100 K/min to reach the specific temperature and kept at that temperature for 1 h. When the crystallization process had completed, the samples were heated to 453 K at a rate of 10 K/min to measure the melting temperature.

Morphology

To characterize the morphology of the blends, the samples were fractured in liquid nitrogen and examined with scanning electron microscope (HITACHI, S-3500). TEM observations are performed on a JEOL JEM 1200-EX TEM with an accelerating voltage of 80 kV.

RESULTS AND DISCUSSION

Morphological characteristics

Figure 1 shows the SEM micrographs of the fractured surface roughly normal to the extrusion direction. There is no phase separation in HDPE/manPE blend as shown in Figure 1(a); it suggests that manPE is compatible with HDPE. As can be seen in Figure 1(b), the blend exhibits obvious aggregation of $CaCO_3$ particles; it seems that the nanoscaled $CaCO_3$ particles could not be dispersed well in the HDPE/$CaCO_3$ blend. Figure 1(c) shows the SEM micrograph of HDPE/manPE/$CaCO_3$ and the $CaCO_3$ particles are hardly distinguishable from the HDPE matrix. Figure 2 gives the TEM image of HDPE/manPE/$CaCO_3$ and shows that the particles are well dispersed in the matrix. The manPE act as a

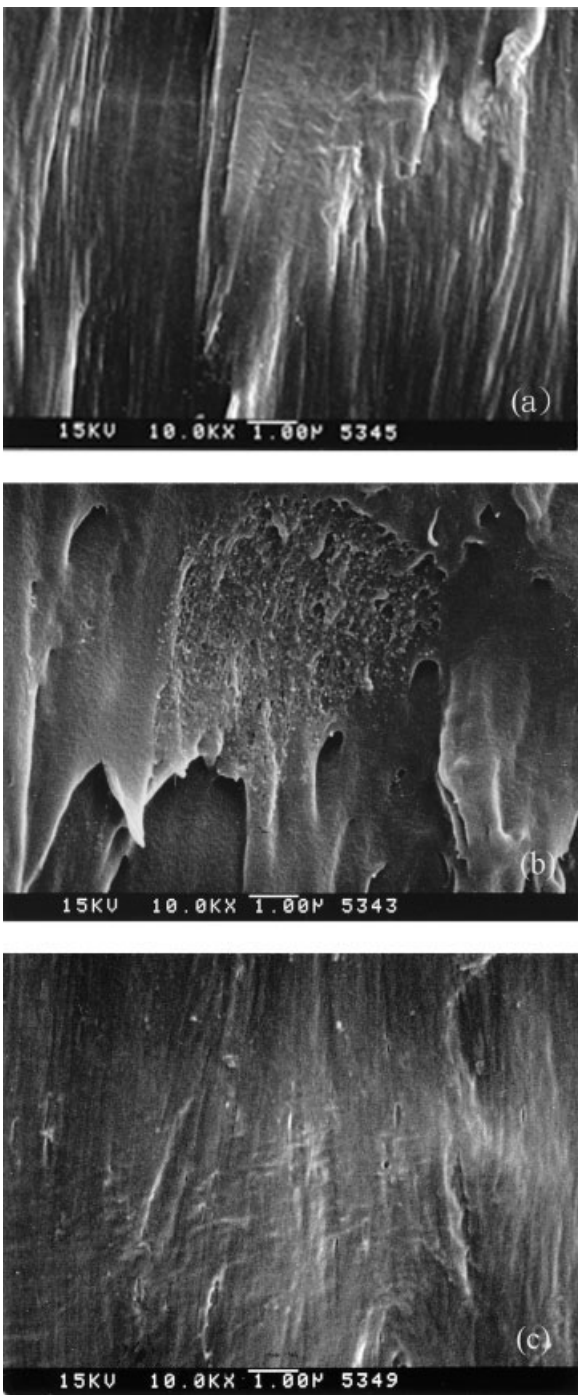

Figure 1 SEM micrograph of HDPE blends. (a) HDPE/manPE; (b) HDPE/$CaCO_3$; (c) HDPE/manPE/$CaCO_3$.

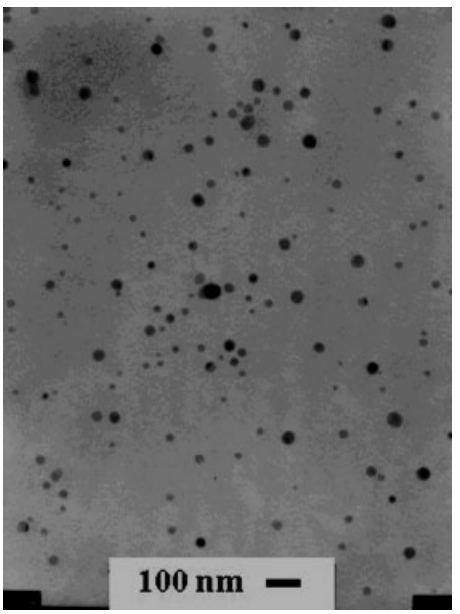

Figure 2 TEM micrograph of HDPE/manPE/$CaCO_3$ blends.

compatibilizer to improve the dispersability of the nanoscaled $CaCO_3$ particles in the blend and effectively prevent particles from aggregation.

Isothermal crystallization

The isothermal crystallization behaviors of the neat HDPE and HDPE blends with different compositions (HDPE/manPE, HDPE/$CaCO_3$, and HDPE/manPE/$CaCO_3$) were investigated with DSC. The isothermal crystallization curves for all samples at different crystallization temperatures (T_c) are plotted in Figure 3. A sample with higher crystallization temperature requires a longer time to complete crystallization. Relative crystallinity (X_t) was calculated as the ratio of the exothermic peak areas at time t and infinite time[14–17]:

$$X_t = \frac{\int_0^t \left(\frac{dH_c}{dt}\right) dt}{\int_0^\infty \left(\frac{dH_c}{dt}\right) dt} \quad (1)$$

where dH_c is the enthalpy of crystallization released during an infinitesimal time interval dt. Figure 4(a–d)

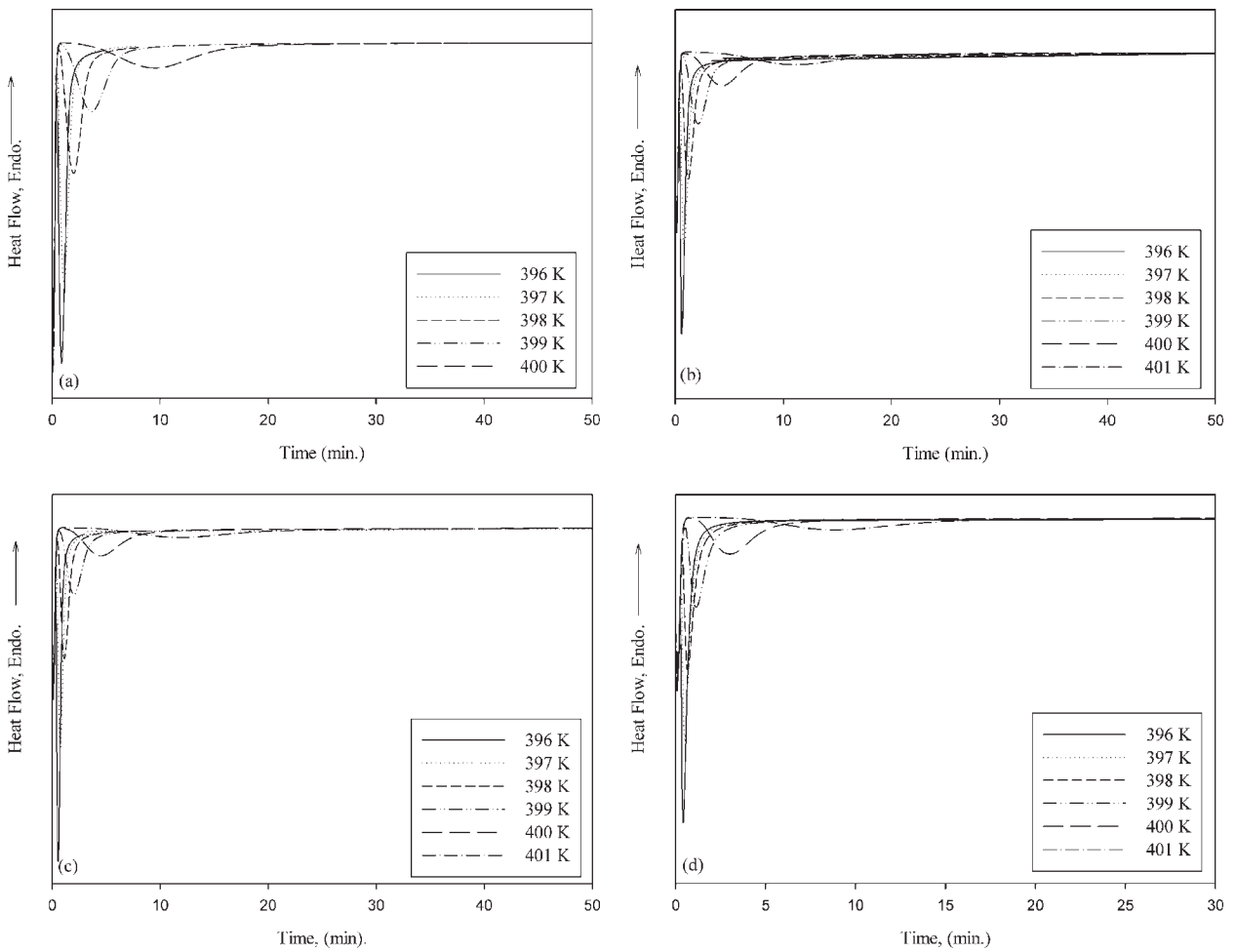

Figure 3 DSC isothermal measurement curves for HDPE, HDPE/manPE, HDPE/$CaCO_3$, and HDPE/manPE/$CaCO_3$ blends. (a) HDPE; (b) HDPE/manPE; (c) HDPE/$CaCO_3$; (d) HDPE/manPE/$CaCO_3$.

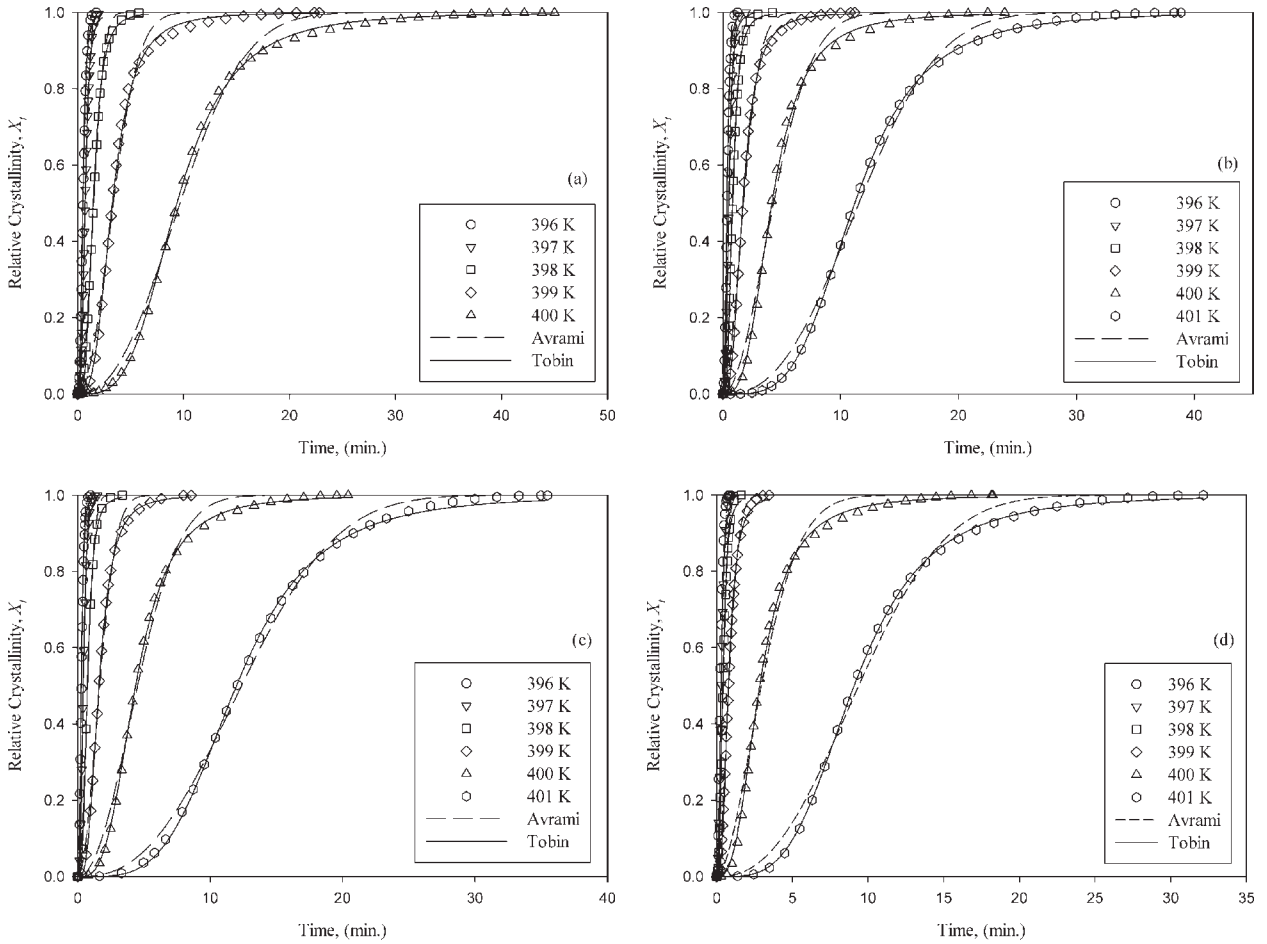

Figure 4 Relative crystallinity as a function of crystallization temperature. (a) HDPE; (b) HDPE/manPE; (c) HDPE/$CaCO_3$; (d) HDPE/manPE/$CaCO_3$.

show the relative crystallinity of neat HDPE and HDPE blends. It could be readily seen that the crystallization kinetics is strongly temperature dependent, and time to complete crystallization obviously increases with increasing T_c within the experimental regime. From these curves, the half-time of crystallization $t_{1/2}$, defined as the time required to reach half crystallinity ($X_t = 0.5$) can be computed. In general, $t_{1/2}$ or $1/t_{1/2}$, is taken as a measure of the overall rate of crystallization of a polymer as shown in Table I. It can be seen that $t_{1/2}$ of all four samples increases with the increasing T_c, which indicates that the total crystallization time is lengthened and that the crystallization rate decreases with increasing T_c.

Avrami analysis

A generally accepted model in studying the crystallization kinetics of polymers is the Avrami theory.[18–20] By assuming that the relative crystallinity increases with an increase in the crystallization time t, the Avrami equation can be used to analyze the isothermal crystallization process of polymers:

$$X_t = 1 - \exp(-(K_a t)^{n_a}) \quad (2)$$

where X_t is the relative crystallinity, t is crystallization time, K_a is the Avrami crystallization rate constant, and n_a is the Avrami exponent. X_t can be calculated from eq. (1). Values of K_a and n_a were found by fitting experimental data of X_t to eq. (2) and the results were shown in Table I. The regression coefficients listed in Table I show that the fitting between the data and model is good.

Avrami exponent (n_a) represents a parameter revealing the nucleation mechanism and growth dimension. For HDPE, and HDPE blends, the n_a values observed are around 2.0–2.5 (Table I). No evident changes of the values of n_a with the addition of manPE or $CaCO_3$ are noticed. Therefore, it may be reasonable to consider that the addition of manPE or $CaCO_3$ do not affect the geometric dimension of HDPE crystal growth. The n_a is close to 2, which meant the crystallization is two-dimensional growth of the lamellae.[21]

While n_a may be considered as a constant with crystallization temperatures (T_c), K_a depends

TABLE I
Kinetic Parameters of Models and Half Time

	Avrami		Tobin			Half time		
T_c (K)	K_a (min^{-1})	n_a	R^2	K_t (min^{-1})	n_t	R^2	$t_{1/2}$	$1/t_{1/2}$
HDPE								
396	1.656	2.09	0.9989	2.046	3.32	0.9998	0.50	1.98
397	1.177	2.25	0.9979	1.433	3.56	0.9989	0.72	1.39
398	0.557	2.28	0.9979	0.676	3.56	0.9992	1.51	0.66
399	0.249	2.08	0.9903	0.307	3.21	0.9987	3.27	0.31
400	0.088	2.32	0.9934	0.107	3.59	0.9996	9.39	0.11
HDPE/manPE								
396	2.303	2.03	0.9985	2.863	3.24	0.9990	0.36	2.80
397	1.623	2.07	0.9991	2.009	3.30	0.9992	0.51	1.96
398	0.984	2.02	0.9982	1.222	3.22	0.9990	0.83	1.20
399	0.469	2.01	0.9923	0.591	3.10	0.9996	1.70	0.59
400	0.185	2.00	0.9894	0.229	3.07	0.9989	5.23	0.19
401	0.070	2.31	0.9956	0.084	3.61	0.9999	14.89	0.07
HDPE/$CaCO_3$								
396	2.897	2.14	0.9990	3.567	3.89	0.9994	0.29	3.50
397	1.942	2.24	0.9992	2.368	3.54	0.9992	0.43	2.32
398	1.102	2.16	0.9983	1.352	3..42	0.9990	0.75	1.33
399	0.498	2.01	0.9943	0.619	3.19	0.9998	1.62	0.62
400	0.192	2.09	0.9925	0.241	3.29	0.9996	4.34	0.23
401	0.075	2.44	0.9972	0.089	3.89	0.9994	12.03	0.08
HDPE/manPE/$CaCO_3$								
396	3.432	2.09	0.9991	4.375	2.99	0.9992	0.23	4.30
397	2.695	2.12	0.9990	3.397	3.05	0.9993	0.30	3.34
398	1.927	2.05	0.9991	2.428	3.06	0.9995	0.42	2.38
399	1.009	2.08	0.9976	1.275	3.01	0.9989	0.79	1.26
400	0.273	2.06	0.9978	0.350	2.98	0.9994	2.81	0.36
401	0.091	2.14	0.9954	0.110	3.55	0.9998	9.03	0.11

strongly on T_c. The isothermal rate constant, K_a, is also shown in Table I as a function of T_c for four samples. It can be seen that the values of K_a, crystallization rates increase with decreasing T_c.

The regression coefficients listed in Table I show that the fitting between the data and model is good. Reconstruction of the relative crystallinity as a function of time for each temperature (as shown in Fig. 4) by using K_a and n_a obtained from Avrami model shows good consistency between the data and the model (eq. (2)) only below $X_t = 0.85$. Avrami model overestimates the experimental data at higher X_t and may be attributed to the impinging effect.

Tobin analysis

The Avrami analysis is only appropriate for early stages of crystallization. To improve the Avrami equation at the later stages of crystallization, a theory of phase transformation kinetics with growth site impingement was proposed by Tobin[22]:

$$X_t = \frac{(K_t t)^{n_t}}{1 + (K_t t)^{n_t}} \quad (3)$$

where K_t is the Tobin rate constant, and n_t is the Tobin exponent. Tobin exponent (n_t) need not be and integer and is mainly governed by different types of nucleation and growth mechanisms. Tobin crystallization parameters (K_t and n_t) can be found by fitting the X_t data obtained for each crystallization temperatures to eq. (3) and the results are shown in Table I. Tobin exponent n_t is found to range from 3.05 to 3.89. The Tobin crystallization rate constant K_t is found to increase with decreasing crystallization temperature, suggesting an increasing crystallization rate with decreasing crystallization temperature.

Comparison between the results obtained from the Avrami and Tobin models (as listed in Table I) shows that both K_t and n_t are greater than K_a and n_a at a specified crystallization temperature. Taking the average of the difference between the two values, $n_t \approx n_a + 1.20$, which is accordance with observation by other studies.[23,24] Tobin model seems to give a better prediction than the Avrami model from regression coefficient (R^2) as listed in Table I. The reconstructed relative crystallinity as a function of time for Tobin model is shown in Figure 3 along with experimental data. It is apparent from Figure 4 that Tobin model provided an excellent fit to the experimental data throughout the range.

Equilibrium melting temperature

The equilibrium melting temperature (T_m^o) of a polymer is an important thermodynamic parameter of

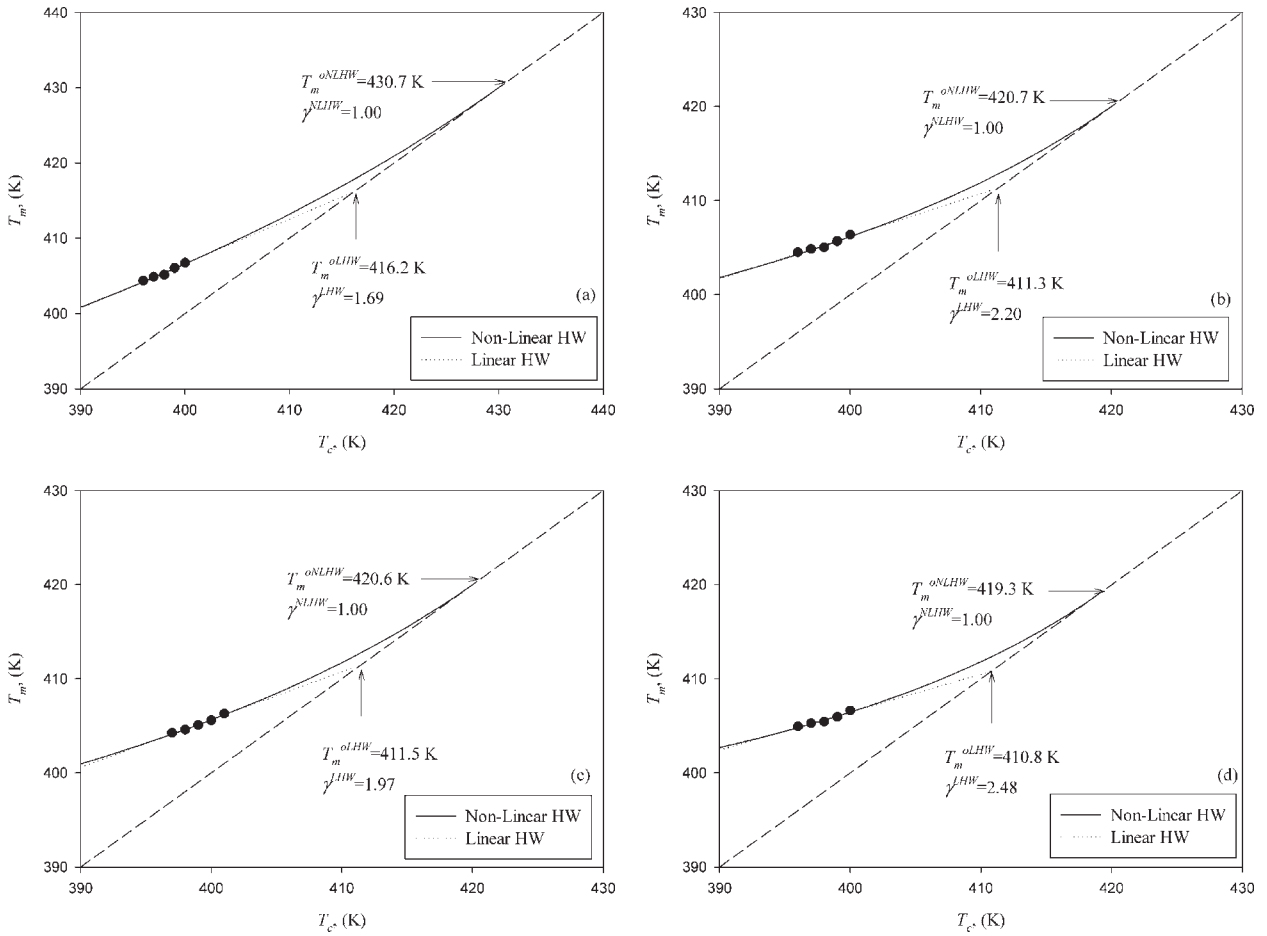

Figure 5 T_m^o obtained from linear and nonlinear HW plots for (a) HDPE; (b) HDPE/manPE; (c) HDPE/$CaCO_3$; (d) HDPE/manPE/$CaCO_3$.

crystallizable chain polymers, as it is the reference temperature for the driving force of crystallization.[25,26] T_m^o of a polymer crystal is defined as the melting temperature of an infinite stack of extended chain crystals, large in directions perpendicular to the chain axis and where the chain ends have established an equilibrium state of pairing.

Several methods had been used to estimate the equilibrium melting temperature.[25–28] Hoffman–Weeks relation[28] has been extensively accepted to estimate equilibrium melting temperature (T_m^o), which can be determined by extrapolation of T_m versus T_c to $T_m = T_c$ (called linear HW):

$$T_m' = T_m^{\mathrm{oLHW}}\left(1 - \frac{1}{\gamma^{\mathrm{LHW}}}\right) + \frac{T_c}{\gamma^{\mathrm{LHW}}} \qquad (4)$$

The thickening coefficient $\gamma^{\mathrm{LHW}} = l/l^*$, where l and l^* are the lamellar thickness at the time of melting and the thickness of the critical nucleus at T_c, respectively.[29] T_m is observed melting temperature and T_c is crystallization temperature. Figure 5(a–d) show the plots of the T_m versus T_c for HDPE, HDPE/manPE, HDPE/$CaCO_3$, and HDPE/manPE/$CaCO_3$, and the equilibrium melting temperature (T_m^{oLHW}) and γ^{LHW} calculated from linear HW are also shown in Figure 5. Linear HW analysis gave γ^{LHW} values of 1.69, 2.20, 1.97, and 2.48 respectively, for HDPE, HDPE/manPE, HDPE/$CaCO_3$, and HDPE/manPE/$CaCO_3$, which are physically meaningless as it would imply rapid and significant thickening of polymer lamellae at very short time after their formation. The basic assumption of the linear HW is that the thickening coefficient γ^{LHW} for lamellae is independent of T_c and time, and there is linear relation between observed T_m and T_c. This assumption has been showed to underestimate the equilibrium melting temperature and overestimate thickening coefficient.[30–33]

Alamo et al.[30] have explained the nonlinearity in the observed T_m and T_c. l^* should be dependent on the degree of undercooling ($\Delta T = T_m - T_c$) and $l^* = C_1/\Delta T + C_2$, where C_1 and C_2 are constant. But C_2 is always ignored in linear HW. On the basis of thermodynamics, Gibbs–Thomson equation[25,26] is an important theory to estimate the equilibrium melting

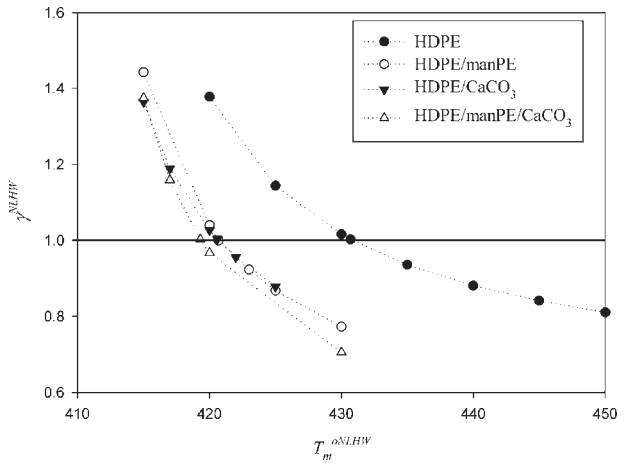

Figure 6 Calculated thickening coefficients at different specific equilibrium melting temperature.

temperature, but some limitations to the theory have been raised.[31,34] Marand and coworkers[31,32] have derived, from Gibbs–Thomson equation, a nonlinear Hoffman–Weeks equation (NLHW):

$$M = \gamma\left(\frac{\sigma_e^l}{\sigma_{em}}\right)(X + a) \tag{5}$$

$$M = \frac{T_m^{\mathrm{oNLHW}}}{T_m^{\mathrm{oNLHW}} - T_m} \tag{5a}$$

$$X = \frac{T_m^{\mathrm{oNLHW}}}{T_m^{\mathrm{oNLHW}} - T_c} \tag{5b}$$

$$a = \frac{\Delta H_f C_2}{2\sigma_e^l} \tag{5c}$$

where T_m^{oNLHW} and γ^{NLHW} are the equilibrium melting temperature and thickening coefficient from the nonlinear Hoffman–Weeks equation, σ_e^l is the interfacial energy associated with the basal plane of the mature crystallite, σ_{em} is the fold surface free energy associated with a nucleus of critical size including the extra lateral surface energy due to fold protrusion and the mixing entropy associated with stems of different lengths, and ΔH_f is the heat of fusion of crystal. σ_e^l is assumed to be equal to σ_{em} for most cases.[30] According to eq. (5), the plot of M versus X should give a constant γ^{NLHW} for a specified T_m^{oNLHW}. Figure 6 shows the variation with the value chosen for the equilibrium melting temperature. The ''true'' equilibrium melting temperature (T_m^{oNLHW}) by this method is found when $\gamma^{\mathrm{NLHW}} = 1$. The relations of T_m and T_c from nonlinear HW are also shown in Figure 5 for comparison with linear HW. Nonlinear HW analysis gave T_m^{oNLHW} values of 430.7, 420.7, 420.6, and 419.3 K, respectively, for HDPE, HDPE/manPE, HDPE/$CaCO_3$, and HDPE/manPE/$CaCO_3$. There is apparent difference between the linear HW and nonlinear HW, the nonlinear HW estimate being higher in all samples.

The equilibrium melting temperature of a crystalline polymer is defined as the melting temperature of a perfect crystal formed by infinite molecular weight chains. Either T_m^{oLHW} or T_m^{oNLHW} of HDPE blends were lower than that of neat HDPE; it means that the crystalline of HDPE in HDPE blends was less perfect than that of pure HDPE.

To compare the crystallization ability, undercooling should be taken into consideration since the crystallization rate of a polymer depends mainly on its undercooling ($T_m^{\mathrm{oNLHW}} - T_c$).[35] The undercooling and crystallization rate constants calculated from the Tobin model and $1/t_{1/2}$ are shown in Figure 7. All four samples shows similar trend that the crystallization rate constants increase with increasing undercooling indicating higher crystallization rate at greater undercooling. At a specific value of rate constant, HDPE/manPE/$CaCO_3$ needs to be imposed the lowest undercooling, followed by HDPE/$CaCO_3$, HDPE/manPE, and HDPE; it indicates that the crystallization rate follows the order: HDPE/manPE/$CaCO_3$ > HDPE/$CaCO_3$ > HDPE/manPE > HDPE. The overall crystallization rate is governed by nucleation and diffusion.[36] The maleic anhydride groups of manPE might associate through some interactions such as hydrogen bonding to form effective nuclei to enhance crystallization.[37] Inorganic $CaCO_3$ is an effective nucleation agent and will induce heterogeneous nucleation to enhance crystallization of polymer.[4] The nanosized $CaCO_3$ particles are well dispersed in HDPE/manPE/$CaCO_3$, and form more nuclei to induce a faster crystallization.

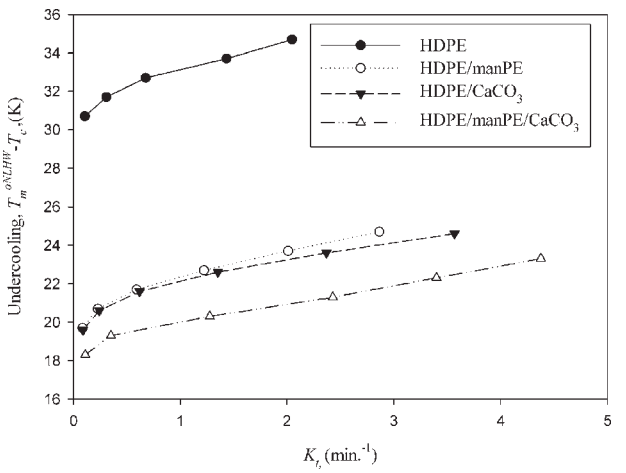

Figure 7 Relation of undercooling and rate constants evaluated from Tobin model (K_t).

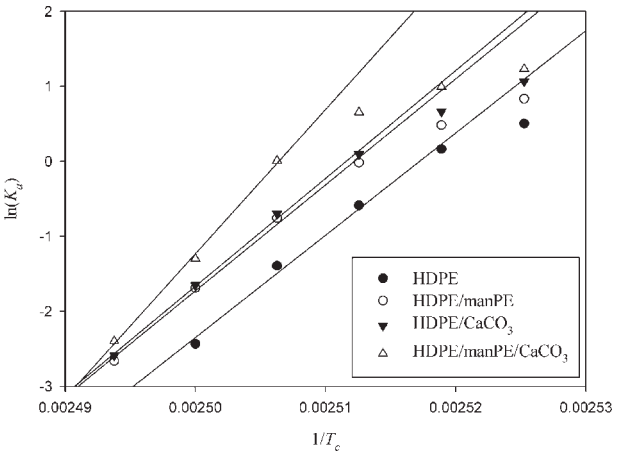

Figure 8 Plots of ln K_a as a function of $1/T_c$.

Activation energy (ΔE)

The crystallization process is assumed to be thermally activated and the crystallization rate constant K_a can be approximately described as follows:

$$\ln K_a = \ln K_0 - \frac{\Delta E}{RT_c} \tag{6}$$

where K_0 is the temperature-dependent pre-exponential factor, R is the gas constant, and ΔE is the activation energy for the primary crystallization process, which consists of the transport activation energy and the nucleation activation energy. Plots of ln K_a against $1/T_c$ for HDPE and HDPE blends are shown in Figure 8. The plots are linear only at higher crystallization temperatures for all four samples. Similar results were also observed in polyethylene/montmorillonite nanocomposites.[4] The activation energy was determined from the slope of the plots and the obtained values were 136, 141, 143, and 192 KJ/mol for HDPE, HDPE/manPE, HDPE/$CaCO_3$, and HDPE/manPE/$CaCO_3$, respectively, as shown in Table II. The activation energy of HDPE/manPE/$CaCO_3$ is higher than those of the other three. As mentioned above, the more dispersed $CaCO_3$ particles act as nucleating agents and the nucleation effect of the more dispersed $CaCO_3$ particles on crystallization of HDPE is stronger in the HDPE/manPE/$CaCO_3$ than the other samples. The activation energy (ΔE) contained the transport activation energy and the nucleation activation energy. Therefore, it is believed that the higher activation energy in HDPE/manPE/$CaCO_3$ is due to higher transport activation energy because the dispersed particles would retard the molecular mobility.[4]

Lauritzen and Hoffman theory

The overall crystallization rate should be interpreted by the combination of nucleation and growth phenomena. Hoffman and Lauritzen[38] propose the following equation:

TABLE II
The Activation Energy for the Primary Crystallization, Nucleation Constants, and Fold Surface Free Energy of HDPE and HDPE Blends

	ΔE (KJ/mole)	$K_g \times 10^{-5}$ (K^2)	σ_e (J/m^2)
HDPE	136	3.49	3.19
HDPE/manPE	141	1.59	1.49
HDPE/$CaCO_3$	143	1.57	1.47
HDPE/manPE/$CaCO_3$	192	1.36	1.30

$$\psi(T_c) = \psi_0 \exp\left[\frac{-U^\star}{R(T_c - T_\infty)} - \frac{K_g}{T_c(\Delta T)f}\right] \tag{7}$$

where $\psi(T_c)$ is crystallization rate parameter and ψ_0 is a pre-exponential term; U^* = 1500 cal/mol is the diffusional activation energy for the transport of crystallizable segments at the liquid-solid interface; R is the gas constant; $T_\infty = T_g - 30$ K is the hypothetical temperature below which viscous flow ceases; T_g is glass transition temperature of HDPE and T_g = 163 K.[39] $\Delta T = T_m^o - T_c$; $f = 2\,T_c/(T_m^o + T_c)$ is a correction factor; K_g is the nucleation parameter that can be related to the product of lateral (σ) and folding surface free energy (σ_e).

The crystallization rate parameter $\psi(T_c)$ could be considered proportional to $1/t_{1/2}$, eq. (7) can be rewritten as:

$$\frac{1}{t_{1/2}} = \psi_0 \exp\left[\frac{-U^\star}{R(T_c - T_\infty)} - \frac{K_g}{T_c(\Delta T)f}\right] \tag{8a}$$

or

$$\ln\left(\frac{1}{t_{1/2}}\right) + \frac{U^\star}{R(T_c - T_\infty)} = \ln\psi_0 - \left(\frac{K_g}{T_c(\Delta T)f}\right) \tag{8b}$$

Figures 9 and 10 shows the plot of eq. (8b) for HDPE, HDPE/manPE, HDPE/$CaCO_3$, and HDPE/

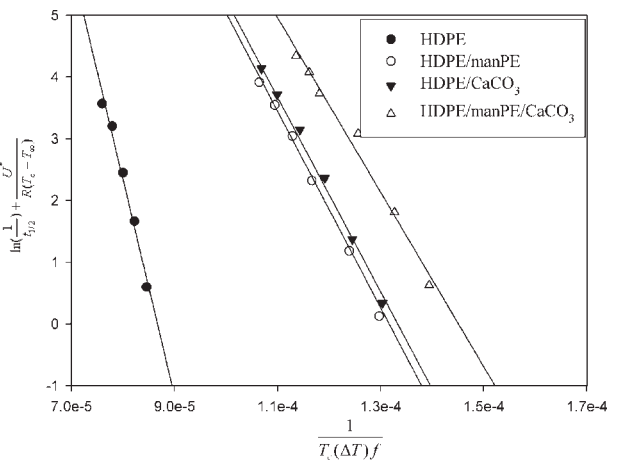

Figure 9 Lauritzen–Hofmann plots for isothermal crystallization of HDPE and HDPE blends.

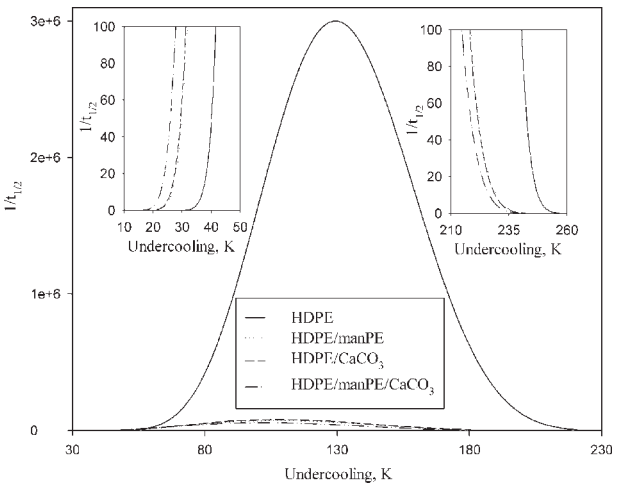

Figure 10 The fitted curves drawn through the data after eq. (8a) ($T_m^o = T_m^{oNLHW}$).

manPE/$CaCO_3$ by using $T_m^o = T_m^{oNLHW}$. The K_g could be obtained from the slope and intercept of Figure 9 and the results are listed in Table II. Figure 9 exhibits very good linear relation for all four samples and no obvious slope change. The range of T_c studied in this article belonged to regime I of crystallization of HDPE,[1] and the K_g (3.49×10^5 K^2) was close to the value (3.13×10^5 K^2) obtained from regime I in previous studies.[1] The obtained K_g values can be used to determine the fold surface free energy (σ_e)[38]:

$$K_g = \frac{4b\sigma\sigma_e T_m^o}{k\Delta h_f} \quad \text{(regime I)} \tag{9}$$

where b is the width of the chain, 4.11×10^{-10} m for HDPE[40]; $\sigma = 1.07 \times 10^{-2}$ J/m^2 for HDPE[41]; k is the Boltzman constant, and Δh_f is the enthalpy of fusion.[42] The fold surface free energy (σ_e) was estimated by eq. (9) and listed in Table II. The incorporation of nucleating agents into polymers could lead to a reduction of the value of σ_e, thereby giving rise to an increase of the crystallization rate. The lower values of σ_e in HDPE blends than neat HDPE are associated with the nucleating agent additions.[43–45] The addition of $CaCO_3$ particles or maleic anhydride groups would act as nucleating agents to increase the nucleation rate. The σ_e value of HDPE/manPE/$CaCO_3$ composites is smaller than the other three samples. A lower σ_e implies more heterogeneous nucleation in HDPE/manPE/$CaCO_3$ blend, which contained more dispersed $CaCO_3$ particles as a result of good dispersion.

By taking the T_m^o calculated from nonlinear HW ($T_m^o = T_m^{oNLHW}$) to eq. (8b), the undercooling ($T_m^o - T_c$) dependence of rate function ($1/t_{1/2}$) could be obtained as shown in Figure 9. At lower undercooling (higher T_c), the crystallization rate is controlled by nucleation and the crystallization rate followed the order: HDPE/manPE/$CaCO_3$ > HDPE/$CaCO_3$ > HDPE/manPE > HDPE, similar to the ranking obtained from Figure 7. The dispersed $CaCO_3$ particles or malic anhydride groups would induce the nucleation to increase crystallization rate.

On the other hand, at higher undercooling (lower T_c) the order of crystallization rate is: HDPE > HDPE/manPE > HDPE//$CaCO_3$ > HDPE/manPE/$CaCO_3$ (as shown in Fig. 9), contrary to the order at lower undercooling. It might be due to the presence of dispersed $CaCO_3$ particles or malic anhydride groups would retard the molecular mobility to crystallize and the crystallization rate is controlled by molecular diffusion at higher undercooling. Because of experimental limitations, crystallization rate at higher undercooling could not be measured. However, the fact that HDPE/manPE/$CaCO_3$ blend had higher active energy seemed to support such interpretation.

CONCLUSIONS

The nanoscaled $CaCO_3$ particles are well dispersed in HDPE with manPE as a compatibilizer. The isothermal crystallization kinetics of HDPE and HDPE blends were investigated by DSC and described by Avrami and Tobin model. Tobin model showed a better simulation in the entire range of X_t. The presence of well-dispersed $CaCO_3$ particles or maleic anhydride groups would act as nuclei to induce heterogeneous nucleation and enhance crystallization rate at lower undercooling (higher T_c); on the other hand the $CaCO_3$ particles or maleic anhydride groups seems to confined the HDPE chains to hinder the crystallization at higher undercooling (lower T_c).

References

1. Tjong, S. C.; Bao, S. P. J Polym Sci Part B: Polym Phys 2005, 43, 253.
2. Zhai, H.; Xu, W.; Guo, H.; Zhou, Z.; Shen, S.; Song, Q. Eur Polym J 2004, 40, 2539.
3. Gopakumar, T. G.; Lee, J. A.; Kontopoulou, M.; Parent, J. S. Polymer 2002, 43, 5483.
4. Lin, Z.; Huang, Z.; Zhang, Y.; Mai, K.; Zeng, H. J Appl Polym Sci 2004, 91, 2443.
5. Avella, M.; Cosco, S.; DiLorenzo, M. L.; DiPace, E.; Errico, M. E.; Gentile, G. Eur Polym J 2006, 42, 1548.
6. Zhang, J.; Ding, Q. J.; Zhou, N. L.; Li, L.; Ma, Z. M.; Shen, J. J Appl Polym Sci 2006, 101, 2437.
7. Yiping, H.; Guangmei, C.; Zhen, Y.; Hongwu, L.; Yong, W. Eur Polym J 2005, 41, 2753.
8. Zhang, F.; Qiu, W.; Yang, L.; Endo, T.; Hirotsu, T. J Appl Polym Sci 2003, 89, 3292.
9. Chan, C. C.; Wu, J.; Li, J. X.; Cheung, Y. K. Polymer 2002, 43, 2981.
10. Xie, T.; Liu, H.; Ou, Y.; Yang, G. J Appl Polym Sci 2006, 101, 3361.
11. Fornes, T. D.; Paul, D. R. Polymer 2003, 44, 3945.
12. Kamal, M. R.; Edward, C. Polym Eng Sci 1983, 23, 7.
13. Ma, C. C.; Rong, M. Z.; Zhang, M. Q.; Friedrich, K. Polym Eng Sci 2005, 45, 529.

14. Lewis, C. L.; Spruiell, J. E. J Appl Polym Sci 2006, 100, 2592.
15. Hay, J. N.; Sabir, M. Polymer 1969, 10, 203.
16. Hay, J. N.; Fitzgerald, P. A.; Wiles, M. Polymer 1976, 17, 1015.
17. Hay, J. N. Brit Polym J 11: 137 1979.
18. Avrami, M. J Chem Phys 1939, 7, 1103.
19. Avrami, M. J Chem Phys 1939, 8, 212.
20. Avrami, M. J Chem Phys 1939, 9, 177.
21. Jieping, L.; Zhaobin, Q.; Jungnickel, B. J. J Polym Sci Part B: Polym Phys 2005, 43, 287.
22. Tobin, M. C. J Polym Sci Part B: Polym Phys 1974, 12, 399.
23. Ravindranath, K.; Jog, J. P. J Appl Polym Sci 1993, 49, 1395.
24. Supaphol, P.; Spruiell, J. E. J Macromol Sci Phys 2000, B39, 257.
25. Hoffman, J. D.; Davis, G. T.; Lauritzen, J. I. In Treatise on Solid State Chemistry; Hannay, N. B., Ed.; Plenum: New York, 1976; Vol. 3, Chapter 7.
26. Hoffman, J. D.; Miller, R. L. Polymer 1997, 38, 3151.
27. Flory, P. J.; Vrij, A. J Am Chem Soc 1963, 85, 3548.
28. Hoffman, J. D.; Weeks, J. J. J Res Nat Bur Stand 1962, 66A, 13.
29. Lee, S. W.; Lee, B.; Ree, M. Macromol Chem Phys 2000, 201, 453.
30. Alamo, R. G.; Viers, B. D.; Mandelkern, L. Macromolecules 1995, 28, 3205.
31. Buckley, C. P.; Kovacs, A. J Colloid Polym Sci 1976, 254, 695.
32. Marand, H.; Xu, J.; Srinivas, S. Macromolecules 1998, 31, 8219.
33. Lin, C. C. Polym Eng Sci 1983, 23, 113.
34. Armitstead, K.; Goldbeck-Wood, G. Adv Polym Sci 1992, 100, 219.
35. DiLorenzo, M. L.; Silvestre, C. Prog Polym Sci 1999, 24, 917.
36. Fatou, J. G. Makromol Chem 1984, 7, 131.
37. Seoa, Y.; Kima, J.; Kima, K. U.; Kimb, Y. C. Polymer 2000, 41, 2639.
38. Hoffman, J. D.; Frolen, L. J.; Ross, G. S.; Lauritzen, J. I. J Res NBS 1975, 79A, 671.
39. Gorbunov, V. V.; Fuchigami, N.; Tsukruk, V. V. High Perform Polym 2000, 12, 603.
40. Mezghani, K.; Philips, P. J. Physical Properties of Polymer Handbook; Mark, J. E., Ed.; American Institute of Physics: New York, 1996; Chapter 31.
41. Hoffman, J. D. Faraday Discuss Chem Soc 1979, 68, 378.
42. Brandrup, J.; Immergut, E. H. Polymer Handbook; 3rd ed.; Wiley: New York, 1989.
43. Jiang, X.; Zhang, Y.; Zhang, Y. J Polym Sci Part B: Polym Phys 2004, 42, 1181.
44. Beck, H. N. J Appl Polym Sci 1975, 19, 371.
45. Arroyo, M.; Zitzumbo, R.; Avalos, F. Polymer 2000, 48, 6351.